

Robust electrical spin injection into a semiconductor heterostructure

B. T. Jonker,* Y. D. Park,[†] and B. R. Bennett
Naval Research Laboratory, Washington, DC 20375

H. D. Cheong, G. Kioseoglou, and A. Petrou
State University of New York at Buffalo, Buffalo, New York 14260
 (Received 13 January 2000)

We report efficient electrical injection of spin-polarized carriers from a non-lattice-matched magnetic contact into a semiconductor heterostructure. The semimagnetic semiconductor $\text{Zn}_{1-x}\text{Mn}_x\text{Se}$ is used as a spin-injecting contact on a GaAs-based light-emitting diode. Spin-polarized electrons are electrically injected across the II-VI/III-V interface, where they radiatively recombine in a GaAs quantum well and emit circularly polarized light. An analysis of the optical polarization which includes quantum confinement effects yields a lower bound of 50% for the spin injection efficiency.

Spin injection and transport in semiconductor heterostructures represent a promising avenue to add new spin-dependent functionality to the many attractive properties of semiconductor devices.¹ The seminal proposal by Datta and Das of a spin-polarized field-effect transistor,² with magnetic source and drain contacts for spin injection and detection, has stimulated a great deal of effort to better understand the behavior of spin-polarized carriers in semiconductor hosts under conditions of dynamic transport. Optical pumping has routinely been used to create spin-polarized carrier populations in semiconductor heterostructures and has provided tremendous insight into their behavior.³ Very recently, extraordinarily long spin lifetimes and diffusion lengths have been observed in optically pumped systems:^{4,5} spin diffusion lengths of many micrometers have been reported in GaAs,⁴ for example, illustrating that a spin-polarized mode of operation is certainly feasible for every modern transport device.

It is very desirable to inject spin-polarized carriers *electrically* via a magnetic contact to increase the potential for practical applications. This would provide a very simple and direct implementation of spin injection in which the contact area defines the spin source. Electrical spin injection has been an elusive goal, however. Several attempts using ferromagnetic metal contacts to Si (Ref. 6) or InAs-based two-dimensional electron gas structures^{7,8} have resulted in very similar and modest spin injection effects measured at or below the 1% level. Such small effects make it difficult to either unambiguously confirm spin injection or successfully implement new device concepts. Spin scattering at the interface between the magnetic contact and semiconductor host appears to be the limiting factor, but very little is known about such interfacial contributions. Schmidt *et al.* have recently suggested that the large mismatch in conductivities precludes the use of a common ferromagnetic metal as a spin-injecting contact to a semiconductor based on a classical diffusion-equation-based model.⁹

Oestreich *et al.* previously proposed the use of a Mn-based diluted magnetic (or semimagnetic) *semiconductor* as the spin-injecting contact, which would serve to align the spins of the electrons on a picosecond time scale in an applied magnetic field.¹⁰ They used time-resolved photolumi-

nescence to demonstrate that optically excited carriers became spin aligned in a $\text{Cd}_{1-x}\text{Mn}_x\text{Te}$ layer, and that spin-polarized electrons were transferred into an adjacent CdTe layer with little loss in spin polarization.

We report here robust and efficient electrical injection of spin-polarized carriers from a non-lattice-matched semimagnetic semiconductor contact into a semiconductor heterostructure. This is demonstrated by the fabrication of a spin-polarized light-emitting diode¹¹ (spin-LED) structure based on a GaAs quantum well. In a normal LED, electrons and holes recombine in the vicinity of a *p-n* junction or quantum well to produce light when a forward bias current flows. This light is unpolarized, because all carrier spin states are equally populated, and all dipole-allowed radiative transitions occur with equal probability. In a spin-LED,¹¹ carriers are electrically injected from a contact with a net spin polarization into a semiconductor heterostructure where they radiatively recombine. Radiative recombination of spin-polarized carriers results in the emission of right (σ^-) or left (σ^+) circularly polarized light along the surface normal as given by well-known selection rules.^{3,12} We observe a maximum circular polarization of 50% at 4.2 K. Polarization analysis of the electroluminescence (EL) effectively interrogates the spin polarization of the carriers involved. Thus the existence of circularly polarized EL demonstrates successful electrical spin injection, and an analysis of the circular polarization using these selection rules provides a quantitative assessment of injection efficiency.

As this manuscript was submitted, similar results were published by Fiederling *et al.*,¹³ who also utilized this semimagnetic semiconductor spin-aligner concept¹⁰ to demonstrate efficient electrical spin injection from the lattice-matched quaternary $\text{Be}_{0.07}\text{Mn}_{0.03}\text{Zn}_{0.9}\text{Se}$ into an $\text{Al}_{0.03}\text{Ga}_{0.97}\text{As}/\text{GaAs}/\text{Al}_{0.03}\text{Ga}_{0.97}\text{As}$ LED structure. They report a maximum circular polarization of 43% at 2.5 K, and derive an electron spin polarization of 86% if the light hole/heavy hole (LH/HH) splitting induced by confinement in their 150 Å GaAs quantum well is neglected (this splitting is calculated to be ~ 3 meV). In the work reported here, we use a simpler ternary alloy ($\text{Zn}_{0.94}\text{Mn}_{0.06}\text{Se}$) for the spin-injecting contact with a lattice mismatch of 0.5%, a relatively

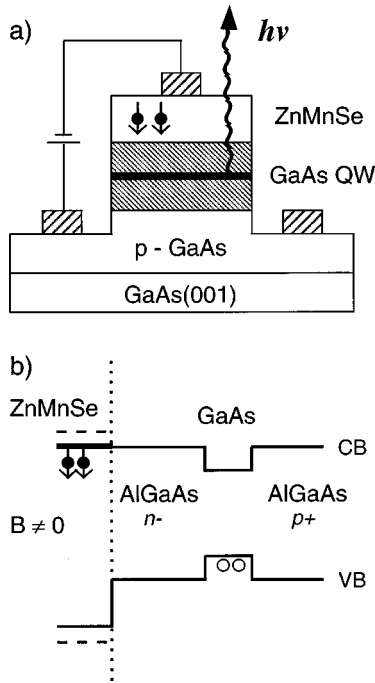


FIG. 1. (a) Schematic cross section of the samples (not to scale). (b) Flat band diagram illustrating the conduction- and valence-band (CB, VB) offsets in the spin-LED structure. The CB of the $\text{Zn}_{0.94}\text{Mn}_{0.06}\text{Se}$ splits with applied field, so that the spin-down states are occupied. The holes in the GaAs quantum well are unpolarized. The band offsets are exaggerated for clarity.

large mismatch in semiconductor heterostructures. Our results demonstrate that efficient electrical spin injection is not limited to perfectly lattice-matched structures, and therefore is widely applicable in more common heteroepitaxial systems. In addition, we explicitly consider the effects of the LH/HH splitting resulting from quantum confinement. This splitting is calculated, experimentally measured, and included in the data analysis, resulting in a *lower bound* of 50% for the electrical spin injection efficiency. These results are very encouraging for the future realization of magneto-electronic devices.^{1,2}

A cross section of the spin-LED layered structure is shown in Fig. 1(a). An epilayer of the II-VI semimagnetic semiconductor $\text{Zn}_{1-x}\text{Mn}_x\text{Se}$ is used as the spin-injecting contact to a (III-V)-based LED structure, which consists of a GaAs quantum well flanked by $\text{Al}_y\text{Ga}_{1-y}\text{As}$ barrier layers. Semimagnetic semiconductors are well studied, and noted for the very large band-edge spin splitting they exhibit in an applied magnetic field (giant effective Zeeman effect).¹⁴ For modest fields, the spin splitting significantly exceeds $k_B T$ at low temperature. In particular, the splitting of the spin-up ($m_j = +\frac{1}{2}$) and spin-down ($m_j = -\frac{1}{2}$) electron states in $\text{Zn}_{0.94}\text{Mn}_{0.06}\text{Se}$ is ~ 10 meV at 3 T, so that the conduction band effectively forms a completely polarized source of spin-down electrons. This same effect has been used in the past to create a static spin superlattice, in which carriers of opposite spin occupy alternating layers of a multilayer structure.¹⁵ Under appropriate bias, these carriers are electrically injected across the ZnMnSe/AlGaAs heterointerface and into the GaAs quantum well, where they radiatively recombine with an unpolarized hole population provided by *p*-type doping, and emit circularly polarized light.

The samples studied were grown on semi-insulating GaAs(001) substrates by molecular-beam epitaxy (MBE) in a multichamber system. The growth sequence (Fig. 1) consisted of a $1 \mu\text{m}$ *p*-type GaAs buffer layer, a 500 \AA *p*-doped AlGaAs barrier, an undoped 150 \AA GaAs quantum well, and an *n*(Si)-doped 500 \AA AlGaAs barrier. Dopant setbacks of 250 \AA were used on either side of the well, and $p(\text{Be}) = 10^{18} \text{ cm}^{-3}$. A 2000 \AA epilayer of *n*(Cl)-doped $\text{Zn}_{0.94}\text{Mn}_{0.06}\text{Se}$ was grown in a second attached MBE chamber. This growth was initiated by exposing the (2×4) -As reconstructed surface of the AlGaAs to the Zn flux for 60 s at the growth temperature of $300 \text{ }^\circ\text{C}$ to minimize the formation of defects near the interface.¹⁶ For these growth conditions, the ZnSe/GaAs conduction-band (CB) offset is 100 meV ,¹⁷ with the ZnSe band edge at higher energy. The band gap of $\text{Zn}_{0.94}\text{Mn}_{0.06}\text{Se}$ is nearly equal to that of ZnSe (2.8 eV at 4.2 K) due to band-gap bowing, while that of AlGaAs increases with Al concentration. An Al concentration of 0.1 was chosen for the barrier to minimize the ZnMnSe/AlGaAs CB offset, which is calculated to be $\sim 10 \text{ meV}$, forming a staircase potential profile. The lattice mismatch is 0.5% .¹⁴ A doping level of $n = 10^{17} \text{ cm}^{-3}$ was used for both the AlGaAs and the ZnMnSe to minimize band bending. The depth of the GaAs CB quantum well is $\sim 100 \text{ meV}$. A simplified flat band diagram is shown in Fig. 1(b).

The samples were processed into surface-emitting LED mesas $200\text{--}400 \mu\text{m}$ in diameter using standard photolithographic techniques, and electrical contacts were made to the ZnMnSe and *p*-GaAs base via Ti/Au liftoff. The top mesa contact consists of concentric rings, leaving most of the mesa surface optically transparent. The LED samples were placed in a magnetic cryostat with optical access along the field direction (Faraday geometry), and electrically biased to inject electrons from the ZnMnSe into the GaAs quantum well at current densities of $\sim 0.01 \text{ A/cm}^2$. The surface-emitted EL was measured with a spectrometer using a combination of a quarter-wave plate and linear polarizer for polarization analysis.

Representative spectra of the light emitted from the spin-injected LED are shown in Fig. 2 for selected values of the applied field. The spectra are normalized and aligned to the zero-field spectrum to facilitate comparison. At zero field, no optical polarization is observed, as expected, since $\text{Zn}_{0.94}\text{Mn}_{0.06}\text{Se}$ is a Brillouin paramagnet which acquires a net magnetization only in a magnetic field. The emission peaks near 1.524 eV , attributed to recombination with heavy holes, confirming that radiative recombination occurs in the GaAs quantum well. The polarization rapidly increases with applied field as a spin-polarized electron population is created in the ZnMnSe and injected into the LED structure. The corresponding spectra reveal a significant difference in intensity between the σ^+ and σ^- components of the EL even at 0.5 T . Other effects that might contribute to the optical polarization were carefully considered, and either eliminated or included in the error bars.¹⁸ At $B = 4 \text{ T}$, two distinct features are visible at ~ 2 and 4 meV to the low-energy side of the HH peak, and are consistent with contributions from donor- and acceptor-bound excitons, respectively. These features are more distinct at 8 T , and will be discussed elsewhere. The feature near 1.515 eV is attributed to recombination in bulk GaAs, and also exhibits a strong polarization, indicating that some portion of the spin-polarized electrons retain their spin

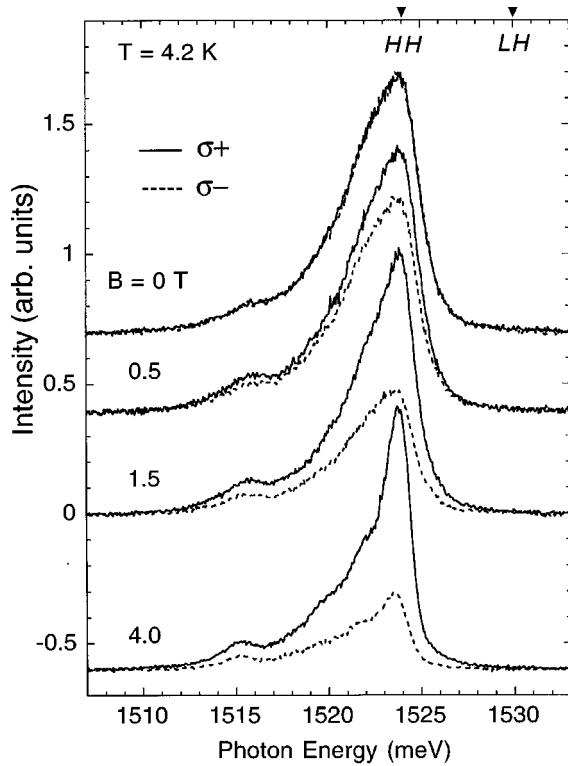


FIG. 2. Electroluminescence spectra from a spin-LED for selected values of applied magnetic field, analyzed for left (σ^+) and right (σ^-) circular polarization. The peaks are normalized and shifted to lower energies by the following amounts to align with the zero-field spectrum: 0.5 T (0.11 meV), 1.5 T (0.61 meV), 4 T (2.15 meV). The relative positions of the heavy- and light-hole features (HH, LH) obtained from photoreflectivity measurements ($B=0$) are indicated.

until they recombine in the p -GaAs buffer layer. It should be noted that the observation of polarization in this dc measurement clearly demonstrates that the electron spin lifetime is much longer than the radiative recombination time.^{4,5}

The degree of circular polarization is obtained from the integrated intensity as $P_{\text{circ}} = [I(\sigma^+) - I(\sigma^-)] / [I(\sigma^+) + I(\sigma^-)]$, and is summarized in Fig. 3 as a function of applied field. P_{circ} saturates around 4 T at a value of 50%, and decreases slightly at the highest fields. This decrease is attributed primarily to the shift of the spin-down ($m_j = -\frac{1}{2}$)

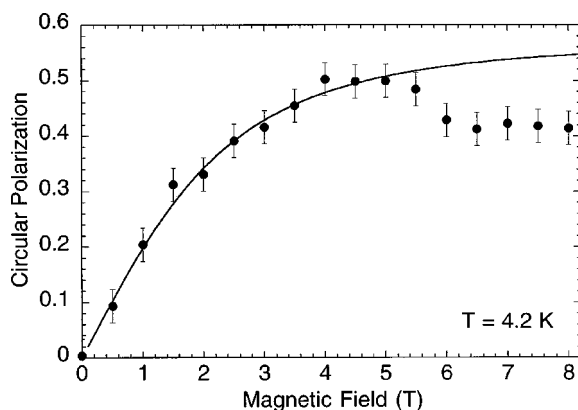


FIG. 3. Magnetic-field dependence of the optical polarization P_{circ} . The solid line is a simple Brillouin function fit to the data.

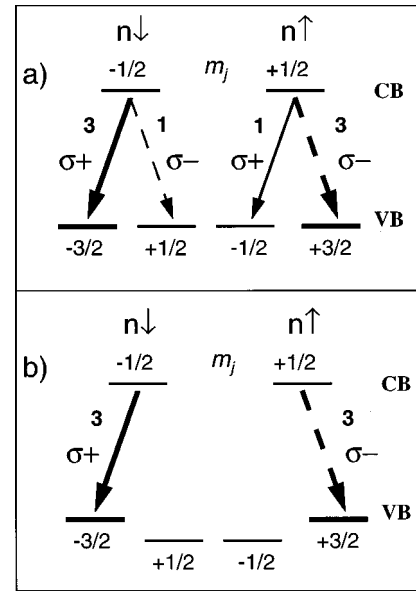


FIG. 4. Radiative interband transitions allowed by the selection rules for the cases of (a) degenerate and (b) nondegenerate HH and LH bands.

$\text{Zn}_{0.94}\text{Mn}_{0.06}\text{Se}$ band below the Fermi level, diluting the initial electron spin polarization, and in part to the Zeeman effect in GaAs, whose spin splitting is much smaller, but opposite in sign to that of $\text{Zn}_{0.94}\text{Mn}_{0.06}\text{Se}$. In a Brillouin paramagnet, the dependence of the magnetization (and spin splitting) on applied field and temperature is well described by a Brillouin function.^{14,19} The solid line in Fig. 3 shows the spin splitting of $\text{Zn}_{0.94}\text{Mn}_{0.06}\text{Se}$ calculated from a standard Brillouin function analysis and scaled by a multiplicative factor to fit the polarization data. The excellent agreement with the field dependence of the circular polarization for $B < 5$ T confirms that the polarization of the EL results from spin-polarized electrons which are electrically injected from the $\text{Zn}_{0.94}\text{Mn}_{0.06}\text{Se}$.

The selection rules that govern the radiative recombination of spin-polarized carriers in cubic semiconductors in the Faraday geometry are illustrated in Fig. 4.^{3,12} They permit a simple analysis of the data which provides a quantitative measure of the spin polarization of the carriers involved, and hence of spin injection efficiency across the ZnMnSe/AlGaAs interface and into the quantum well. In bulk zincblende semiconductors such as GaAs, the conduction band is twofold degenerate at the center of the Brillouin zone, corresponding to spin-up and spin-down electrons ($m_j = \pm \frac{1}{2}$). The valence band is fourfold degenerate, and consists of heavy-hole and light-hole bands with large and small effective mass, respectively, which are each twofold spin degenerate ($m_j = \pm \frac{3}{2}, \pm \frac{1}{2}$). Radiative electron-hole recombination is allowed for interband transitions that obey the selection rule $\Delta m_j = \pm 1$. The probability of a given transition is weighted by the matrix element connecting the levels involved, so that transitions to HH states are three times more likely than those to LH states, as indicated in the figure.

The net circular polarization of the light emitted can readily be calculated for a given occupation of the quantum-well carrier states. Assuming an unpolarized *degenerate* hole population, a general expression for the degree of circular

polarization in the Faraday geometry follows directly from Fig. 4(a), and can be written in terms of the relative populations of the electron spin states $n_{\uparrow}(m_j = +\frac{1}{2})$ and $n_{\downarrow}(m_j = -\frac{1}{2})$, where $0 \leq n \leq 1$ and $n_{\uparrow} + n_{\downarrow} = 1$:

$$P_{\text{circ}} = [I(\sigma^+) - I(\sigma^-)] / [I(\sigma^+) + I(\sigma^-)] = 0.5(n_{\downarrow} - n_{\uparrow}) / (n_{\downarrow} + n_{\uparrow}). \quad (1)$$

The optical polarization is directly related to the electron spin polarization $(n_{\downarrow} - n_{\uparrow}) / (n_{\downarrow} + n_{\uparrow})$ in the quantum well, and has a maximum value of 0.5 due to the degeneracy of the HH and LH bands. The measured value $P_{\text{circ}} = 0.5$ suggests spin injection with an efficiency of 100%.

However, the HH and LH bands are separated in energy by quantum confinement, which modifies Eq. (1) and significantly impacts the analysis. The HH/LH band splitting is typically several meV even in shallow quantum wells, and is much larger than the thermal energy at low temperature (~ 0.36 meV at 4.2 K), so that the LH states are at higher energy and are not occupied. For the structures studied here, a calculation that includes corrections for exciton binding energies yields a value of 5 meV for the HH/LH splitting, slightly smaller than the value of 6 meV obtained from photoreflectivity measurements (these positions are indicated in Fig. 2). In this case, only the HH levels participate in the radiative recombination process, as shown in Fig. 4(b), and P_{circ} is calculated as before:

$$P_{\text{circ}} = (n_{\downarrow} - n_{\uparrow}) / (n_{\downarrow} + n_{\uparrow}). \quad (2)$$

P_{circ} is equal to the electron spin polarization in the well, and can be as high as 1.0. Assuming that only spin-down electrons are injected from the ZnMnSe for $B < 5$ T, the experi-

mentally measured value of $P_{\text{circ}} = 0.5$ indicates electrical spin injection with an efficiency of 50%, i.e., half of the spin-down electrons injected from the ZnMnSe reach the GaAs quantum well without experiencing a scattering event that flips their spin. It should be noted that P_{circ} decreases rapidly with higher current densities, indicating that local heating at the ZnMnSe contact metallization is reducing the initial spin polarization, as expected from the strong temperature dependence of a Brillouin paramagnet.¹⁴ Therefore, the value of 50% should be regarded as a *lower bound* to the spin injection efficiency.

In summary, we have demonstrated highly efficient electrical injection of spin-polarized electrons across a II-VI/III-V semiconductor heterointerface, and subsequent transport into a quantum-well LED structure. An efficient spin-LED effectively couples carrier spin with optical polarization, serves as an efficient carrier spin detector, and may enable the transmission of spin- or polarization-encoded information.¹¹ Fabrication of practical devices will benefit from the use of improved contacts and stronger ferromagnets as the spin injector, perhaps including new ferromagnetic semiconductors such as $\text{Ga}_{1-x}\text{Mn}_x\text{As}$.²⁰⁻²² Future systematic studies of such structures promise to elucidate the mechanisms that contribute to spin scattering and provide a better understanding of spin transport in device structures.

This work was supported by the Office of Naval Research in part under Research Project 02101, and the DARPA SPINS program. The authors gratefully acknowledge helpful discussions with B. V. Shanabrook.

Note added in proof: Recent data on similar samples reveal optical polarizations and corresponding spin injection efficiencies of nearly 70%.

*Author to whom correspondence should be addressed. Email address: jonker@nrl.navy.mil

[†]National Research Council Postdoctoral Associate.

¹G. A. Prinz, *Science* **282**, 1660 (1998).

²S. Datta and B. Das, *Appl. Phys. Lett.* **56**, 665 (1990).

³F. Meier and B. P. Zacharenya, *Optical Orientation* (North-Holland, Amsterdam, 1984), Vol. 8.

⁴D. Hagele *et al.*, *Appl. Phys. Lett.* **73**, 1580 (1998).

⁵J. M. Kikkawa and D. D. Awschalom, *Phys. Rev. Lett.* **80**, 4313 (1998).

⁶Y. Q. Jia, R. C. Shi, and S. Y. Chou, *IEEE Trans. Magn.* **32**, 4707 (1996).

⁷P. Hammer, B. R. Bennett, M. J. Yang, and M. Johnson, *Phys. Rev. Lett.* **83**, 203 (1999).

⁸S. Gardelis *et al.*, *Phys. Rev. B* **60**, 7764 (1999).

⁹G. Schmidt *et al.*, *Phys Rev B* (to be published).

¹⁰M. Oestreich *et al.*, *Appl. Phys. Lett.* **74**, 1251 (1999). See also J. Carlos Egues, *Phys. Rev. Lett.* **80**, 5478 (1998), who models transmission through a spin-dependent barrier.

¹¹B. T. Jonker, U.S. Patent No. 5,874,749 (filed 23 June 1993, awarded 23 February 1999 to U.S. Navy).

¹²C. Weisbuch and B. Vinter, *Quantum Semiconductor Structures* (Academic, New York, 1991), Chap. 11. These selection rules

may not be rigorously obeyed in real systems due to imperfections or distortion, but provide an analysis good to first order.

¹³R. Fiederling *et al.*, *Nature (London)* **402**, 787 (1999).

¹⁴J. K. Furdyna and J. Kossut, *Diluted Magnetic Semiconductors*, Vol. 25 of *Semiconductors and Semimetals* (Academic, New York, 1988).

¹⁵W. C. Chou, A. Petrou, J. Warnock, and B. T. Jonker, *Phys. Rev. Lett.* **67**, 3820 (1991); N. Dai *et al.*, *ibid.* **67**, 3824 (1991).

¹⁶L. H. Kuo *et al.*, *Appl. Phys. Lett.* **67**, 3298 (1995); *J. Vac. Sci. Technol. A* **13**, 1694 (1995).

¹⁷R. Nicolini *et al.*, *Phys. Rev. Lett.* **72**, 294 (1994).

¹⁸For example, the Faraday rotation resulting from transmission through the ZnMnSe is negligible due to the very short path length (2000 Å), and because the GaAs emission wavelength is far from that corresponding to the band gap of $\text{Zn}_{0.94}\text{Mn}_{0.06}\text{Se}$. Photoluminescence data from the GaAs quantum well excited with linearly polarized light from the same LED mesa structures used for the EL studies show little polarization, providing a very effective built-in calibration for each mesa.

¹⁹J. A. Gaj, in Ref. 14, p. 286.

²⁰H. Ohno, *Science* **281**, 951 (1998).

²¹M. Oestreich, *Nature (London)* **402**, 735 (1999).

²²Y. Ohno *et al.*, *Nature (London)* **402**, 790 (1999).